IC/91/222

INTERNATIONAL CENTRE FOR
THEORETICAL PHYSICS

SCALING PROPERTIES OF OPTICAL REFLECTANCE FROM QUASI-PERIODIC SUPERLATTICES

Xiang Wu

He-Sheng Yao

and

Wei-guo Feng

INTERNATIONAL ATOMIC ENERGY AGENCY

UNITED NATIONS EDUCATIONAL, SCIENTIFIC AND CULTURAL ORGANIZATION

MIRAMARE-TRIESTE

IC/91/222

International Atomic Energy Agency

and

United Nations Educational Scientific and Cultural Organization

INTERNATIONAL CENTRE FOR THEORETICAL PHYSICS

SCALING PROPERTIES OF OPTICAL REFLECTANCE FROM QUASI-PERIODIC SUPERLATTICES

Xiang Wu *

International Centre for Theoretical Physics, Trieste, Italy,

He–Sheng Yao

Department of Physics, Anqing Teachers Training College,
Anqing, Anhui, People's Republic of China

and

Wei–guo Feng

Pohl Institute of Solid State Physics, Tongji University,
Shanghai 200092, People's Republic of China.

MIRAMARE – TRIESTE

August 1911

* Permanent address: Pohl Institute of Solid State Physics, Tongji University, Shanghai 200092, People's Republic of China.

Abstract

The scaling properties of the optical reflectance from two types of quasi-periodic metal-insulator superlattices, one with the structure of Cantor bars and the other with the structure of Cantorian-Fibonaccian train, have been studied for the region of s-polarized soft x-rays and extreme ultraviolet. By using the hydrodynamic model of electron dynamics and transfer-matrix method, and by taking into account retardation effects, we have presented the formalism of the reflectivity for the superlattices. From our numerical results, we found that the reflection spectra of the quasi-superlattices have a rich structure of self-similarity. The interesting scaling indices, which are related to the fractal dimensions, of the spectra are also discussed for the two kinds of the quasi-superlattices.

1 Introduction

Many of the one-dimensional quasiperiodic systems[1] obtained in real experimental situation are self-similar objects, i.e., the fractals, the geometrical characteristics of which are invariant over scale dilatations. For instance, Cantor triadic bars [2,3], Fibonacci superlattice[4] are the usual structures of such systems. In general, one of the purposes of an experiment is to determine the fractal dimension D, which measures the manner in which the mass M, embedded in a sphere of radius R, increases: $M(R) \cong R^D$.[2] Another procedure to obtain D is to study the variation of the intensity $I(q)$ scattered by a fractal at a wave vector **q**: $I(q) \cong q^{-D}$.[5] which has been used to interpret small-angle scattering experiments.[6]

Recently, we calculated the reflectivities of s-polarized soft x-rays and extreme ultraviolet from multilayered superlattices.[7,8,9,10] From the numerical results for the Fibonacci superlattice[8], we found that except that the calculated reflection spectra are of the interesting self-similarity pattern, some new strongly reflection peaks move to a higher-frequency region compared with the usual periodic superlattice, which stimulates the interest in the study and making of soft x-rays and extreme ultraviolet reflectors.

In this paper, we propose a new model to show self-similar patterns of reflectance spectra of a kind of quasi-period superlattice, the generalized Cantor triadic superlattice (GOSL). From the theoretical calculations for the two special cases of metal-insulator-GOSL (MIGOSL), one superlattice with the structure of Cantor bars (CBSL), and the other with the structure of Cantorian-Fibonacci train (CFSL), we found that the reflectance spectra patterns from an nth generation MIGOSL has a rich structure of self-similarity as a function of wave frequency of the incident s-polarized soft x-rays and extreme ultraviolet, and the reflection spectra density varies according to the power law at a number of fixed points, which is similar to the case of [5].

2 Model structure of GCSL and reflectivity

The GCSL under consideration is generated recursively along z-direction by two elementary media: medium A and medium B, the corresponding localized dielectric functions of which are $\epsilon_A(\omega)$ and $\epsilon_B(\omega)$ respectively. The model structure, as presented in Fig. 1, maps the mathematical rule of the Cantor sequence as follows,[2]

$$C_1 = B_1A_1B_1, \tag{1}$$

$$C_2 = B_2A_2B_2 \equiv C_1A_2C_1, \tag{2}$$

$$\vdots$$

$$C_n = B_nA_nB_n \equiv C_{n-1}A_nC_{n-1}, \tag{3}$$

where $B_n \equiv C_{n-1}$, while A_n is the same medium as layer A_1 but with different thickness,

$$d_{A_n} = (2+\alpha)^{n-1}d_{A_1}, \tag{4}$$

here the parameter α is just the thickness ratio of d_{A_n} to d_{B_n}. The total thickness of an nth generation GCSL is

$$d_{C_n} = (2+\alpha)^n d_{B_1}. \tag{5}$$

The Fractal dimension of our model, according to the definition,[2] is given by

$$D = \frac{\ln 2}{\ln(2+\alpha)}. \tag{6}$$

It is easily to find that when $\alpha = 1$, the GCSL becomes the usual standard Cantor bar superlattice (CBSL) with $D = \ln 2/\ln 3$; when $\alpha = \Lambda \equiv (\sqrt{5}-1)/2$, the structure of GCSL is somewhat like the Fibonacci superlattice. If we substitute A_n by C_{n-2} and B_n by C_{n-3}, it is just the usual Fibonacci superlattice.[4,8] Hereafter, we will call it as Cantorian-Fibonaccian superlattice (CFSL), the fractal dimension of which is $D = \ln 2/\ln(2+\Lambda)$.

The reflectivity for s-polarized soft x-rays and extreme ultraviolet can be obtained directly following the scheme presented in Refs. [7] and [9]. As in Ref. [7], we again assume that the regions $z < 0$ and $z > d_{C_n}$ are vacuum space and the incident wave vector with incident angle θ is $\mathbf{K}_0 = (q, 0, k_0)$, where $k_0 \equiv (\omega/c)\cos\theta$, and $q \equiv (\omega/c)\sin\theta$. Based on the hydrodynamic theory and the transfer-matrix method and by taking account of damping effects to the system of the nth generation GCSL, we can get the reflectivity for s-polarized wave as follows,[9]

$$R = |\frac{Y_N - Y_0}{Y_N + Y_0}|^2, \tag{7}$$

where

$$Y_0 = -\frac{c_{21} - c_{22}Y_N}{c_{11} - c_{12}Y_N}, \tag{8}$$

$$Y_N = k_0/\omega. \tag{9}$$

and c_{ij} is the element of the transfer matrix $\underline{C}_n$ for the nth generation GCSL, which is given by

$$\underline{C}_n = \underline{C}_{n-1}\underline{M}(k_A, d_{A_n})\underline{C}_{n-1} \tag{10}$$

with the initial transfer matrix

$$\underline{C}_1 = \underline{M}(k_B, d_{B_1})\underline{M}(k_A, d_{A_1})\underline{M}(k_B, d_{B_1}), \tag{11}$$

where $\underline{M}(k, d)$ is the transfer matrix for a medium layer of thickness d, which is defined as

$$\underline{M}(k, d) = \begin{bmatrix} \cos kd & i\omega/k \sin kd \\ ik/\omega \sin kd & \cos kd \end{bmatrix}, \tag{12}$$

and k is a z-component of the wave vector in the medium layer, which satisfies the following equation,

$$k_\mu^2 = (\omega/c)^2\epsilon_\mu(\omega) - q^2, \qquad \mu = A, B. \tag{13}$$

3 Numerical results and conclusions

By using the equations presented in Section 2, one can calculate the reflectivity numerically. In this paper, we apply the theory to the case of MIGCSL system.

We consider the elementary layer B_1 as a metal Al film, and A_n as a dielectric medium with $\epsilon_A = 1$. In order to take account of the retardation effect on the reflection, we choose the model dielectric function in the form of the Drude local dielectric function for the layer B_1,

$$\epsilon_B(\omega) = 1 - \frac{\omega_{PB}^2}{\omega^2 + i\omega/\tau}, \tag{14}$$

where τ is the electric relaxation time in the metal Al layers, which is chosen to be of the order of $10^3\omega_{PB}^{-1}$ as adopted in Refs. [8] and [9], and ω_{PB} is the plasma frequency for metal Al,

$$\omega_{PB} = \sqrt{4\pi n_B e^2/m_e}, \tag{15}$$

where n_B is the electron density of metal Al layer B_1, $n_B = 18.1 \times 10^{22} cm^{-3}$, and m_e is the electron mass.

For the case of normal incidence on the MIGCSL, $q = 0$, and $d_{B_1} = 196$Å, which is just the quarter of the plasma wave length λ_{PB} in metal Al, we plotted the two calculated reflectance curves vs frequency on Figs. 2 and 3. Fig. 2 is for the system with special value $\alpha = 1$, the fifth generation metal-insulator CBSL, and Fig. 3 for that of $\alpha = \Delta$, the sixth generation metal-insulator CFSL. From our numerical results, we draw the following conclusions:

(i) For the MIGCSL system, the spectra pattern of the reflectivity of the soft x-rays and ultraviolet has a rich structure of self-similarity, the reflection peaks of which form a Cantorlike set. Due to the remodulation of the reflection intensity, a couple of new peaks move to the position of high frequency, which is beneficial to the reflector design.

(ii) There are a series of scaling points ω^* in the reflection spectra. The reflectivities around those points are approximately of the following scaling equation,

$$R_{n+1}(\omega - \omega^*) = R_n[(2+\alpha)(\omega - \omega^*)]. \tag{16}$$

One can draw this conclusion from Fig. 4, which shows the plot of reflectivities for three generations ($n = 5, 6, 7$) of metal-insulator CBSL at the fixed point $\omega^* = 1.711\omega_{PB}$.

(iii) As n and τ increase, the spectra of reflectivities are composed of an increasing number of frequency bands, which are scale invariant over dilatations of factor $(2+\alpha)$. Fig. 5 is shown for such a situation with $n=8$ at $\omega^*=3.536\omega_{PB}$, the scale of which is $\Lambda^{-2}=2+\Lambda$. With increasing the particular scale of the frequency the special density of the reflection spectra for an nth generation GCSL R_n, which is defined by

$$< R_n >= \frac{1}{\omega-\omega^*}\int_{\omega^*}^{\omega} R_n(\omega')d\omega', \tag{17}$$

varies according to the power law,

$$< R_n > \cong (\omega-\omega^*)^{-D}, \tag{18}$$

Figs. 6 and 7 show the variations of $< R_n >$ for the two cases: $\alpha = 1, \Lambda$, respectively.

Summarzing, we have presented an analogue method for the reflection from a fractal superlattice GCSL. The reflectivity patterns for the s-polarized soft x-rays and extreme ultraviolet possess the same symmetry properties as the real superlattice structure; they exhibit self-similarity because of the nature of the fractal superlattice. Applications to the two kinds of metal-insulator GCSL: CBSL and CFSL have been described in detail. We expect the concerned experiment to test the predicted scaling properties of the present theory.

ACKNOWLEDGMENTS

We gratefully acknowledge many helpful discussions with Dr. Hong Chen and Mr. Nian-hua Liu. Part of this work was supported by the Chinese National Advanced Technology Foundation through grant No. 040-144-05-085. One of the authors (X.W.) would like to thank Professor Abdus Salam, the International Atomic Energy Agency and UNESCO for hospitality at the International Centre for Theoretical Physics, Trieste.

References

[1] P. J. Steinhardt and S. Ostlund, ***The Physics of Quasicrystals***, (World Scientific, Singapore, 1987).

[2] B. B. Mandelbrot, ***The Fractal Geometry of Nature*** (Freeman, New York, 1982).

[3] C. Allain and M. Cloitre, Phys. Rev. B **33**, 3566 (1986); ***Fractal in Physics***, eds., L. Pietronero and Tosatti, (Elsevier Science Publishers B. V., 1986). p. 61.

[4] R. Merlin, K. Bajema, R. Clarke, F. Y. Juang, and P. K. Bhattacharya, Phys. Rev. Lett. **55**, 1768 (1985).

[5] T. A. Witten and L. M. Sander. Phys. Rev. B **27**, 5686 (1983).

[6] D. W. Shaefer, J. E. Martin, D. Cannel, and P. Wiltzius, Phys. Rev. lett. **52**, 2371 (1984); D. W. Shaefer and K. D Keefer, ***ibid*** **53**, 1383 (1984).

[7] Wei-guo Feng, Y. P. He, and Xiang Wu, ***Proc. Workshop on the Physics of Superlattice and Quantum Well*** (World Scientific, Singapore, 1989). p. 190; Acta Optics Sin. **10**, 139 (1990).

[8] Wei-guo Feng, W. He, D. Xue, Y. Xu, and Xiang Wu, J. Phys.: Condensed Matter **1**, 8241 (1989); Wei-guo Feng, He-shen Yao, and Xiang Wu, ***ibid.*** **2**, 6547 (1990).

[9] N. Liu, Wei-guo Feng, and Xiang Wu, Commun. Theor. Phys. **14**, 1 (1990).

[10] W.-g. Feng, N.-h. Liu and X. Wu, Phys. Rev. B43, 6893 (1991).

Figure captions

Fig. 1. Successive stages of generating iterative GCSL: the black bars denote the medium B layers with thickness d_{B_1}; the blank bars denote the medium A layers with $d_{A_n} = (2+\alpha)^{n-1} d_{A_1}, \alpha = d_{A_1}/d_{B_1}$.

Fig. 2. Reflectivity vs ω of a fifth Al-insulator-CBSL ($\alpha = 1$) with $d_{B_1} = \lambda_{PB}/4$ for normal incidence. ω_{PB} and λ_{PB} are the plasma frequency and wave length for metal Al, respectively. $\tau\omega_{PB} = 100$, and $\epsilon_A = 1$.

Fig. 3. Reflectivity for normal incidence on a sixth Al-insulator CFSL ($\alpha = \Lambda \equiv (\sqrt{5}-1)/2$). $d_{A_1} = \Lambda d_{B_1}$. The other relevant parameters are the same as Fig. 2.

Fig. 4. Reflectivities of normal incidence on the three generations of Al-insulator-CBSL C_5, C_6, and C_7. $\omega^* = 1.711\omega_{PB}$ and $\Delta\omega_5 = 0.243\omega_{PB}$. The other relevant parameters are the same as Fig. 2.

Fig. 5. The same as Fig. 3 but with generation $n = 8$ and weaker retardation effect: $\tau\omega_{PB} = 500$. $\omega^* = 3.536\omega_{PB}$ and $\Delta\omega_8 = 0.0142\omega_{PB}$.

Fig. 6. Log-log plot giving the variations of $< R_7 >$ at $\omega^* = 1.711\omega_{PB}$ for the Cantorian triadic metal Al and insulator superlattice. $\Omega \equiv \omega - \omega^*$. The open circles show the calculated data. The relevant parameters are the same as Fig. 2.

Fig. 7. Log-log plot giving the variations of $< R_8 >$ at $\omega^* = 3.536\omega_{PB}$ for the 8th Al-insulator CFSL. The open circles show the calculated data. The relevant parameters are the same as Fig. 5.

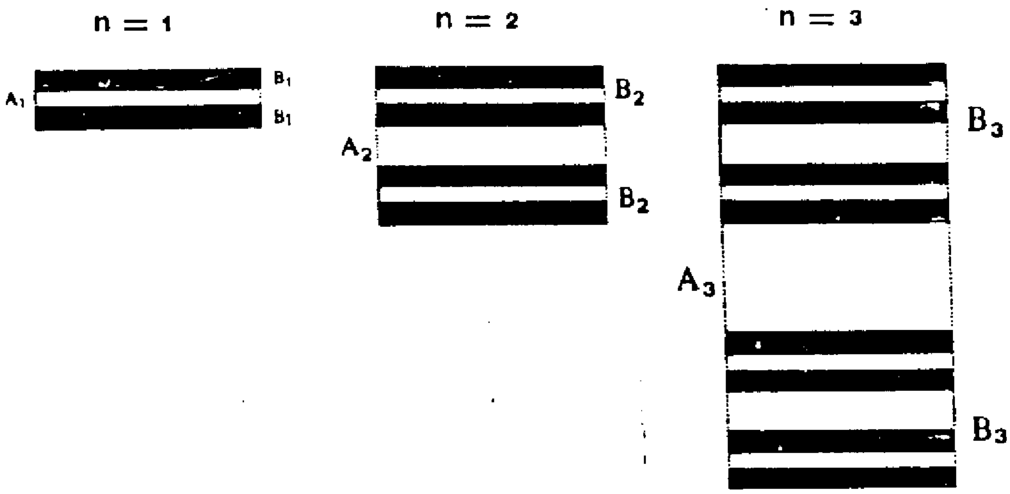

n = 1
n = 2
n = 3
B_1
A_1
B_1
B_2
A_2
B_2
B_3
A_3
B_3

Fig.1

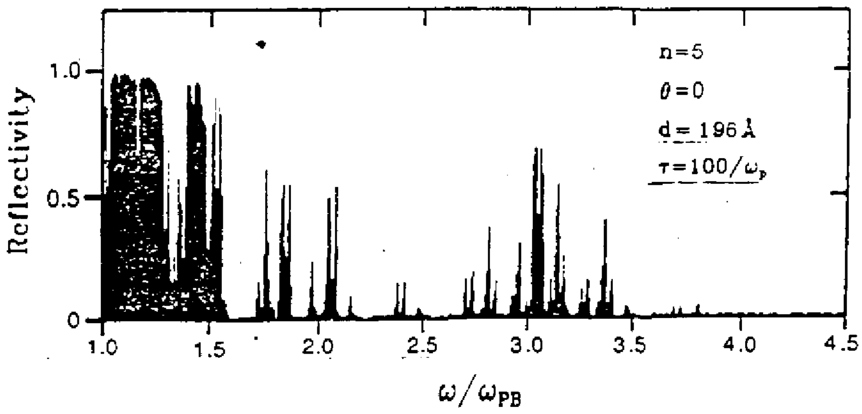

n=5
θ=0
d= 196 Å
τ=100/ω_p
Reflectivity
1.0
0.5
0
1.0
1.5
2.0
2.5
3.0
3.5
4.0
4.5
ω/ω_PB

Fig.2

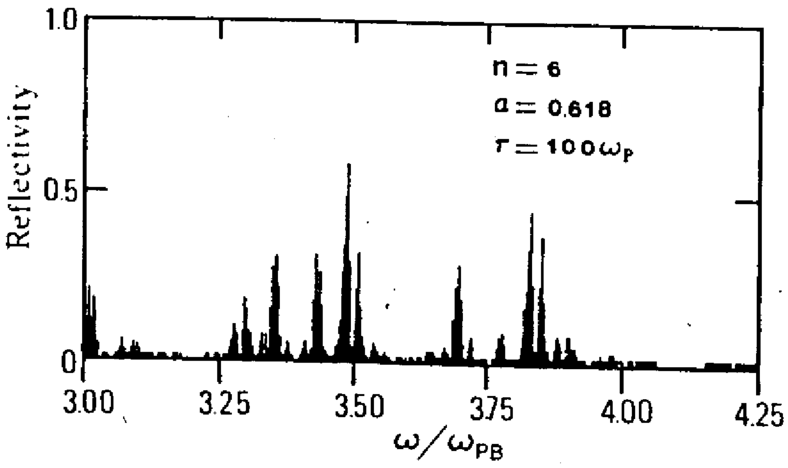

1.0
0.5
0
Reflectivity
n = 6
a = 0.618
τ = 100ωp
3.00
3.25
3.50
3.75
4.00
4.25
ω/ωPB

Fig.3

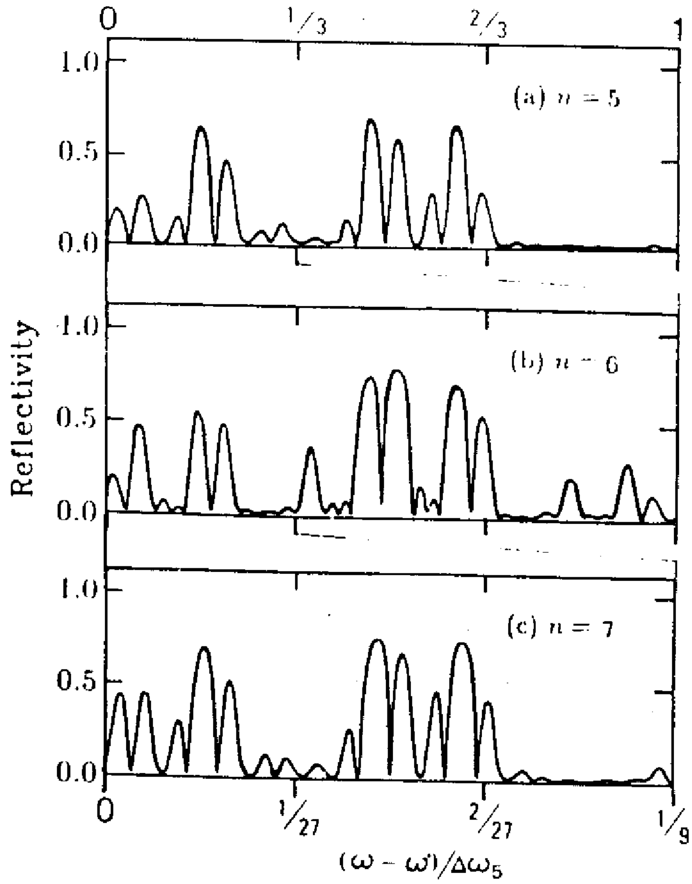

0
1/3
2/3
1
1.0
0.5
0.0
(a) n = 5
(b) n = 6
(c) n = 7
Reflectivity
0
1/27
2/27
1/9
(ω − ω')/Δω5

Fig.4

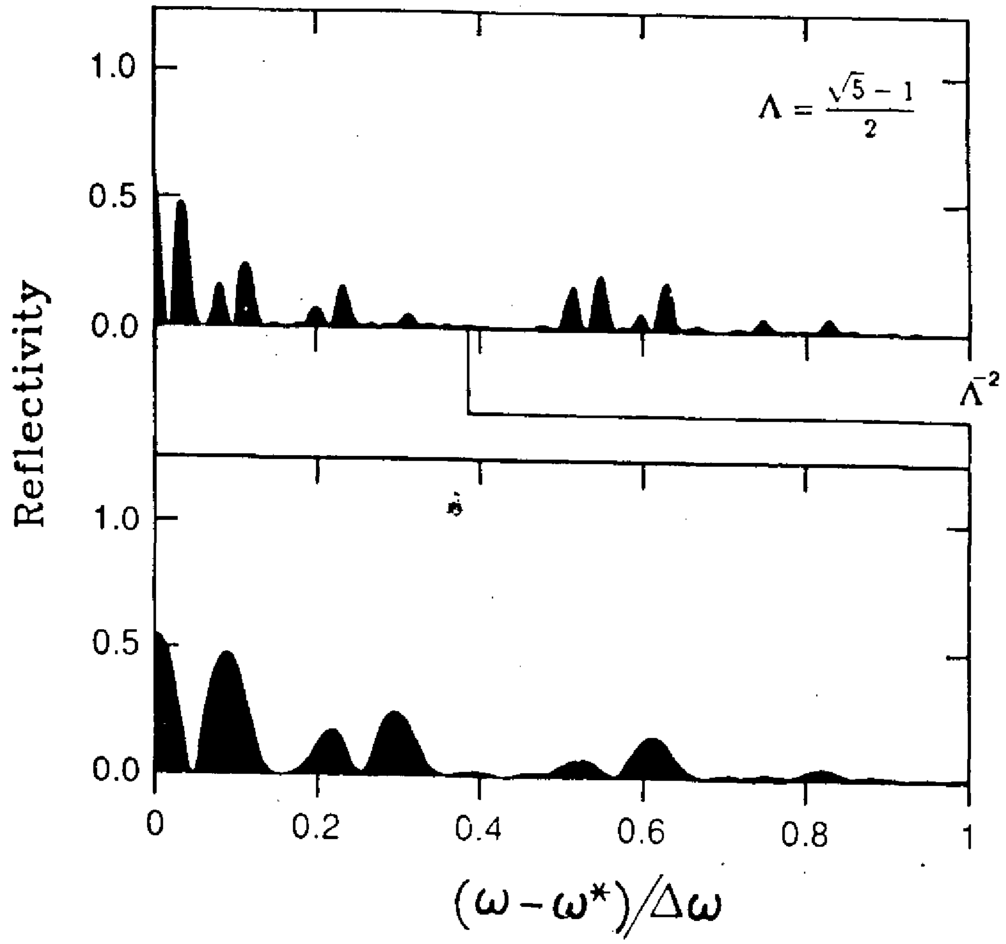
Reflectivity
1.0
0.5
0.0
$\Lambda = \frac{\sqrt{5}-1}{2}$
Λ^{-2}
1.0
0.5
0.0
0
0.2
0.4
0.6
0.8
1
$(\omega - \omega^*)/\Delta\omega$

Fig.5

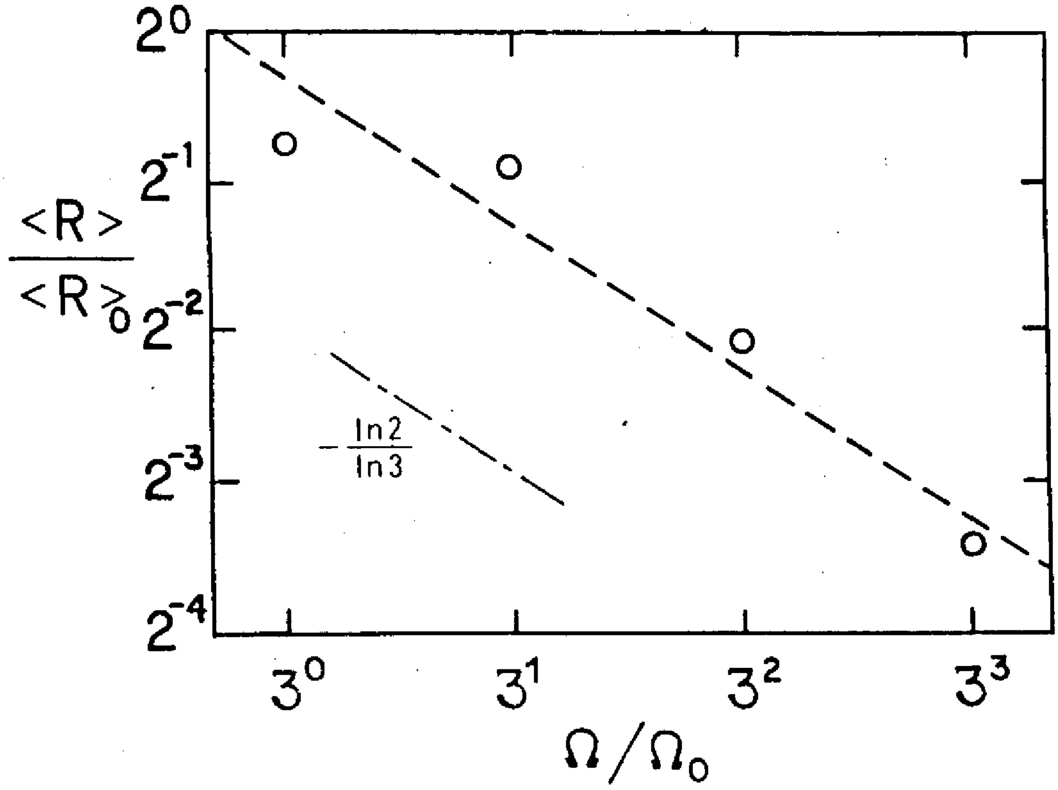

2^0
2^{-1}
2^{-2}
2^{-3}
2^{-4}
$\frac{<R>}{<R>_0}$
$-\frac{\ln 2}{\ln 3}$
3^0
3^1
3^2
3^3
Ω/Ω_0

Fig.6

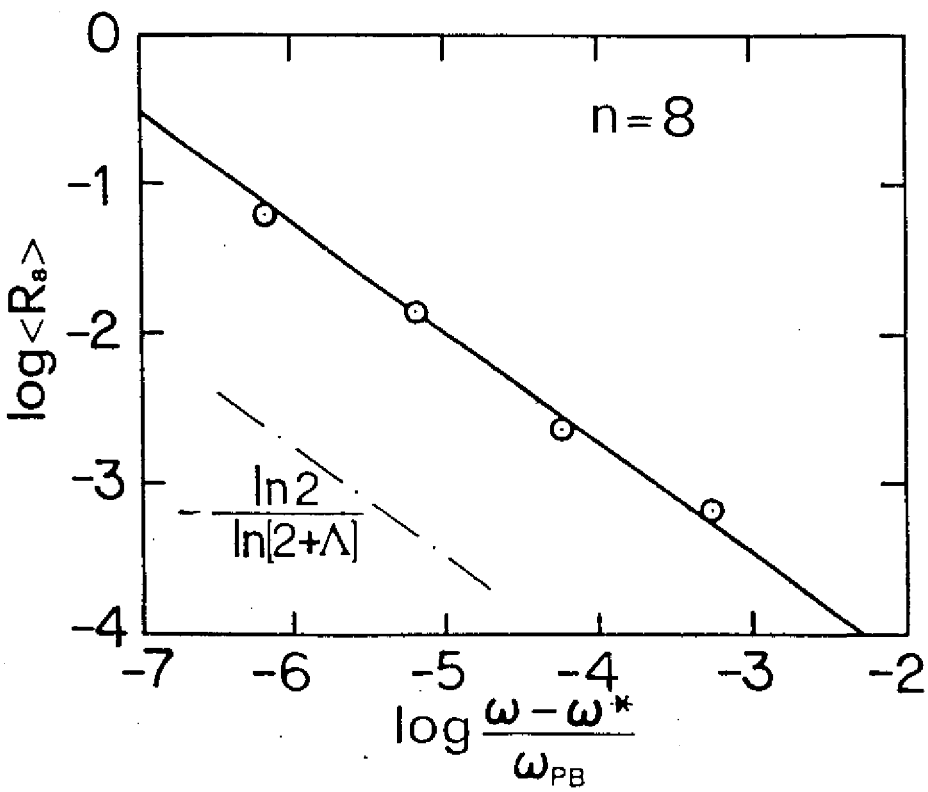

0
-1
-2
-3
-4
n=8
$\log\langle R_a\rangle$
$-\frac{\ln 2}{\ln[2+\Lambda]}$
-7
-6
-5
-4
-3
-2
$\log\frac{\omega-\omega^*}{\omega_{PB}}$

Fig.7